Available online at www.sciencedirect.com

SCIENCE DIRECT®

Computers and Geotechnics 32 (2005) 92–106

COMPUTERS AND GEOTECHNICS

www.elsevier.com/locate/compgeo

Mechanics of a discontinuity in a geomaterial

A.P.S. Selvadurai [*,1], Q. Yu

Department of Civil Engineering and Applied Mechanics, McGill University, 817 Sherbrooke Street West, Montreal, QC, Canada H3A 2K6

Received 16 February 2004; received in revised form 22 September 2004; accepted 20 November 2004

Abstract

The paper presents a brief overview of the topic of interfaces and discontinuities in geomechanics and develops computational assessment of the two-dimensional problem of a discontinuity in a geomaterial region that is subjected to relative shear movement with provision for dilation of the discontinuity. The evaluation focuses on the assessment of the influence of the surface topography of the discontinuity, frictional contact mechanisms, failure of the parent material composing the discontinuity and incompatible movements at the contacting planes on the behaviour of the discontinuity. The computational modelling is used to examine the shearing tests conducted by Bandis et al. [Fundamentals of rock joint deformation. Int J Rock Mech Min Sci Geomech Abstr 1983;20:249–68] on samples of dolerite.

Keywords: Geomaterial discontinuity; Incompatible movements; Material plasticity; Contact mechanics; Hydraulic conductivity of fractures; Mechanics of joint

1. Introduction

The terms interfaces, discontinuities and joints, mean different things to different people and the associated interpretations are generally somewhat subjective. In the context of the study of geomaterials, an interface is regarded as the physical boundary between two dissimilar materials. Examples of these can include the boundary between an inclusion or an aggregate or a reinforcing element encountered in cementitous materials such as concrete or the continuous boundary between different geological horizons. During application of either mechanical or environmental loading, interfaces are generally expected to exhibit complete continuity in both the displacement and tractions. On occasions, the interface can exhibit delaminations leading to the loss of continuity in the mechanical and kinematic responses. Discontinuities on the other hand can occur in both homogeneous and inhomogeneous material regions. The development of a discrete fracture in a brittle fashion in a uniform cementitious material or in a brittle geologic material leads to the development of a discontinuity. Such processes can also introduce the notion of a joint, which usually refers to a new material region contained between two parent materials. While the study of interfaces is important in examining the overall behaviour of geomaterials and geomaterial composites, the study of the behaviour of discontinuities is perhaps of greater importance in view of the complexities of constitutive behaviour that commonly accompanies their mechanical behaviour. The study of the mechanical behaviour of such discontinuities is of significant importance to geomechanics and geotechnical engineering. With either single or multiple discontinuities, the ability for the interface to transfer loads can control the stability and deformability of the geomaterial region. Examples of these can include the behaviour of excavations tunnels in fractured rock, mechanics of reinforcement

* Corresponding author. Tel: +1 514 398 6672; fax: +1 514 398 7361.
E-mail address: patrick.selvadurai@mcgill.ca (A.P.S. Selvadurai).
1 William Scott Professor.

0266-352X/$ - see front matter
doi:10.1016/j.compgeo.2004.11.007

action in rock masses, earth reinforcement and geotechnical construction and mechanics of fractures and faults in seismic zones. Other applications in the context of cementitious geomaterials can include the study of the load transfer through cracks in both reinforced and unreinforced concrete and through discontinuities in brittle ceramics. Other secondary influences of the mechanics of a discontinuity relates to the assessment of its flow and transport characteristics. The examination of these aspects have acquired considerable importance in the context of geoenvironmental engineering involving the study of ground water flow and contaminant transport through discontinuities that evolve with mechanical actions.

The earliest attempts to examine the mechanical behaviour of discontinuities and interfaces are linked to the classical studies of friction between surfaces. Although the history of the study of friction dates back to the works Leonardo da Vinci (1452–1519), Guillaume Amontons (1663–1705) and John Desagulier (1683–1744), the correct interpretation of friction in terms of concepts in mechanics commences with the work of Coulomb [1]. The history of study of the theory of friction between surfaces is also described in the classical treatise by Bowden and Tabor [2] and by Johnson [3]. The theory of frictional phenomena between material surfaces plays a key role in topics related to frictional wear of metallic materials, abrasion effects and degradation of material surfaces induced by wear, microfracture and fragmentation at contacting surfaces. The process of gouge generation in geomaterials has some similarities to the process of abrasion and degradation in metallic materials.

The focus on the study of mechanical behaviour of geomaterial discontinuities has a more recent history initiated largely by interests related to the accurate modelling of laminated and fractured rock masses for geotechnical calculations. An early attempt in this regard relates to the description of the geometrical characteristics of the interface itself. Patton [4] provided a quantitative measure of the roughness of the surface by defining a dilation angle and proceeded to develop a theory for the shear strength of a rock joint based on the measure of its roughness. The work of Ladanyi and Archambault [5] is regarded as a key development in the study of geomaterial discontinuities. In this work, a model for the shear strength of rock joints is developed by assuming that two modes of failure will occur simultaneously. Barton [6] established an empirical law for the description of the shear strength of rock joints, which required the introduction of the concept of a "*joint roughness coefficient*" (JRC) to evaluate the roughness contribution to the generation of shear strength. To aid the calculations, Barton and Choubey [7] also presented roughness profiles and the corresponding JRC values for ten planar roughness profiles. A comparison of the roughness profile of a joint or a fracture was then used to interpret the appropriate JRC value (see also ISRM [8]). The characterization of the surface features of fractures, joints and discontinuities also feature prominently in work related to their physical evaluation. The work of Tse and Cruden [9] interprets the work of Barton and Choubey [7] in the form of an equation. The interpretation of the purely empirical results of Barton and Choubey [7] in terms of statistical parameters and fractal measures have been presented by a number of authors including Reeves [10], Lee et al. [11] and Xie et al. [12]. An important distinction is that, whereas the shear strength of a discontinuity depends on the direction of shearing, the conventional statistical measures and fractal measures are void of a directional property (Huang and Doong [13]; Jing et al. [14]; Seidel and Haberfield [15]). More recent work of Grasselli and Egger [16] considers the three-dimensional surface features of fractures and interfaces and their role in the generalized shear behaviour of rock fractures, joints and interfaces. The characterization of joints and interfaces in terms of fractal measures has been extensively studied (see e.g., Brown and Scholz [17]; Turk et al. [18]; Carr [19]; Lee et al. [11]; Wakabyashi and Fukusighe [20]; Xie and Pariseau [21]). Although physical characterizations of fracture surfaces are quite extensively treated, the development of constitutive models based on such descriptions is rare. Any attempt into the conceptual micro-mechanical modelling of the mechanical behaviour of joints and discontinuities is further complicated by the fact that many of these required characterizations, be it either constitutive, or physical or geometrical are rarely known with the degree of confidence which makes any constitutive model development meaningful. For example recent studies into surface topography characterizations of fractures and joints have achieved mathematical descriptions of surface topographies with considerable precision (Gentier et al. [22]). Whether such representations can truly address issues pertaining to the identification of mechanical behaviour of joints at various scales of practical interest, remains to be seen. The work of Davis and Salt [23] deals with the analytical characterization of undulating shears surfaces in rock. Kodikara and Johnston [24] have examined the behaviour of rock-concrete interfaces in connection with the study of the load carrying capacity of rock-socketed piers. The studies by Armand et al. [25,26] deal with the shear behaviour of artificially smoothed discontinuities composed of marble and natural discontinuities of granodiorite. The work of Yang and Chiang [27] deals with an experimental study of the progressive shear behaviour of rock discontinuity with tooth-shaped asperities. While most of the work described previously relate to the mechanics of discontinuities and interfaces in geological media deal with virgin surfaces, importance of infill material such as gouge and debris in influencing the mechanical behaviour of the discontinuity has been appreciated in a number of works including the earlier studies by Brekke [28], Brekke and Selmer-Olsen [29], Bernaix [30], Romero [31] and Schnitter and Schneider [32]. Another systematic study by Goodman [33] investigated the strength and deformability characteristics of filled joints, which also established the effect of the thickness of the filling on the behaviour of the joint. A further study by Tulinov and Molokov [34] also examined a similar problem, where the amplitude of the irregularities in the joint surface was small in comparison to the size of the sheared area. These experimental results were also repeated by Goodman et al. [35], who also investigated the influence of pore fluid generation in such joint regions containing infill with low hydraulic conductivity.

The development of experimentation and conceptualization of the mechanical response of geomaterial interfaces was complemented by the development of computational approaches to the modelling of geomaterial interfaces and joints. In the early approaches to such modelling the finite element featured prominently. The earliest application of finite element techniques to the study of rock joints is due to Goodman et al. [35], who developed a model for the mechanics of jointed rocks. In this approach, the joint is treated as a thin layer interface element with non-linear material properties. The thin joint region together with the bounding surfaces exhibited continuous deformations and the non-linear responses were represented through the relative displacements at the planar surfaces composing the interface layer. Due to the two-dimensional and planar nature of the modelling of the interface, the classes of interface problems that could be examined were largely restricted to planar or axisymmetric domains. A number of other investigators including, Zienkiewicz et al. [36], Mahtab and Goodman [37], Fredriksson [38], Ghaboussi et al. [39], Herrmann [40], Pande and Sharma [41], Katona [42], Selvadurai and Faruque [43], Desai [44], Desai et al. [45] and Desai and Nagaraj [46] have conducted investigations related to the application of the thin layer concept to the study of the geomaterial interface problem. The notion of dilatancy of the interface during shear is a characteristic feature of geomaterial interfaces. This aspect was also investigated computationally by Goodman and Dubois [47], Heuze and Barbour [48], Leichnitz [49], Carol et al. [50], Gens et al. [51], Boulon and Nova [52], Aubry and Modaressi [53] and Hohberg [54] employing finite element techniques. The work of Plesha [55], Hutson and Dowding [56], Plesha et al. [57], Qiu et al. [58] and Nguyen and Selvadurai [59] deal with the important aspect of asperity degradation of interfaces during dilatancy and shear of geomaterial interfaces and joints. Results of further investigations are also given by Indraratna and Haque [60]. Other computational modelling of geomaterial interfaces, joints and discontinuities relate to the application of boundary element techniques. In addition to the study of frictional contact problems, Andersson [61], Crotty and Wardle [62], Selvadurai and Au [63] and Selvadurai [64] and Beer and Poulsen [65] have applied boundary element techniques to the examination of geomaterial interfaces and discontinuities with a variety of classes of non-linear material phenomena including, dilatancy and degradation during shear.

Fluid transport characteristics of geomaterial discontinuities are of current importance particularly in connection with geoenvironmental applications that require the study of fluid movements in both the discontinuity and through the intact parent material. Early investigations in this area are due to Snow [66] who examined the influence of the externally applied normal and shear stresses on the alterations in the hydraulic conductivity of a fracture. Other investigations by Brace [67], Kranz et al. [68], Raven and Gale [69], Walsh [70], Engelder and Scholz [71], Gale [72], Haimson and Doe [73], Bandis et al. [74], Pyrak-Nolte et al. [75], Teufel [76], Billaux and Gentier [77], Makurat et al. [78], Tsang [79], Boulon et al. [80], Wei and Hudson [81], Stephansson [82] and Indraratna and Ranjith [83] also examine similar influences of mechanical actions at a discontinuity or an interface on its resulting hydraulic properties. The recent article by Hopkins [84] summarizes the role of joint or interface deformations on the behaviour of rock masses, which ultimately has an influence on the aperture development and its hydraulic behaviour. The work of Nguyen and Selvadurai [59] also extend the concepts to the consideration hydraulic conductivity evolution during interface asperity degradation and accumulation of gouge material. The subject of the mechanics of geomaterial discontinuities and geomaterial interfaces in general have been extensively studied over the past three decades, and useful accounts and reviews of theoretical, experimental and computational developments can be found in the publications by Selvadurai and Voyiadjis [85], Barton and Stephansson [86], Barenblatt et al. [87], Evans and Wong [88], Hudson [89], Selvadurai and Boulon [90], Rossmanith [91], Bandis et al. [92] and Drumm et al. [93].

In the case of geomaterial discontinuities, the experimentation is both difficult and expensive and this presents an opportunity for the application of computational methodologies to conduct *numerical experiments* with a view to identifying features of both the discontinuity and the mode of deformation that influences its shear behaviour. The purpose of this paper is not to develop an all-encompassing approach to the micro-mechanical modelling of the joint, but to consider certain aspects that are perceived to be of interest to the development of phenomenological models of the mechanical and hydraulic behaviour of the discontinuity. Furthermore, attention is restricted to the examination of a plane discontinuity or a profile, which by itself, is recognized as a limitation of the study. The features considered within the general scope of computational modelling included the following: the surface profile of the discontinuity, the contact interaction between the faces of the discontinuity, the incompatible movements at the discontinuity, the plasticity of the parent material constituting the discontinuity, the sense of relative movement of the discontinuity in the presence of a defined surface profile and the stress/stiffness constraints applicable to deformability of the material regions constituting the discontinuity. Many of these features can be easily accommodated for by currently available general-purpose computational codes; in this study, however, we employ the ABAQUS code. Attention is further restricted to the study of a typical discontinuity profile similar to that is provided in the study by Bandis et al. [92] in connection with rock joint characterization.

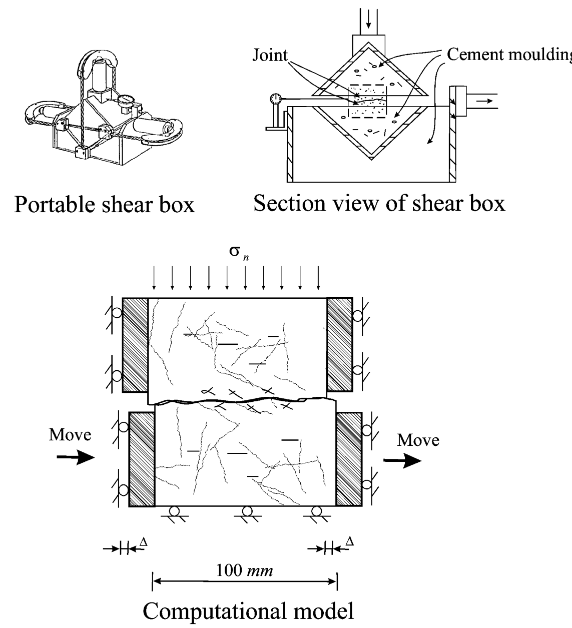

Fig. 1. Experimental and computational models and boundary conditions (After Bandis et al. [92]).

2. Computational modelling

The objective of this paper is to present a brief account of certain aspects of the computational modelling procedures that were adopted for the examination of the incompatible shear behaviour of a discontinuity in a geomaterial.

2.1. The geometry and constraints

The physical problem being modelled is that of an *initially compatible profile* or a *mated-discontinuity* in a block of geomaterial. The geometry of the plane region is dictated by considerations of the size of the sample of dolerite rock tested by Bandis et al. [92]. Considering the fact that this is a well-documented, well-discussed and often-cited test, by modern standards it represents somewhat of a rudimentary testing scheme. For example, it is not altogether clear as to whether the rate of loading and the ability of the separate material regions of the discontinuity to undergo rotation are in any way controlled. There are more complex testing methodologies that have been developed in recent literature, but for the purposes of this paper we shall restrict attention to the study by Bandis et al. [92]. The segments of the rock composing the discontinuity are embedded in a concrete moulding material. Again, it is not altogether clear as to whether separation occurs between the rock sample and the bedding material during the application of the shear loading.

The schematic view of the two-dimensional model of the discontinuity, the boundary and displacement constraints used in the computational modelling are shown in Fig. 1. The upper half of the specimen is restrained against global rotation but permitted to experience rigid body displacements in the "vertical" direction in situations where only vertical loads are applied. There is complete bonding between the rigid plates and the dolerite. The lower half of the specimen is again bonded to the rigid plates and only horizontal displacements are permitted. In the computational modelling, the method of loading is displacement controlled, although it is not quite clear as to whether this is indeed the case in the actual experiments. In the experiments, the

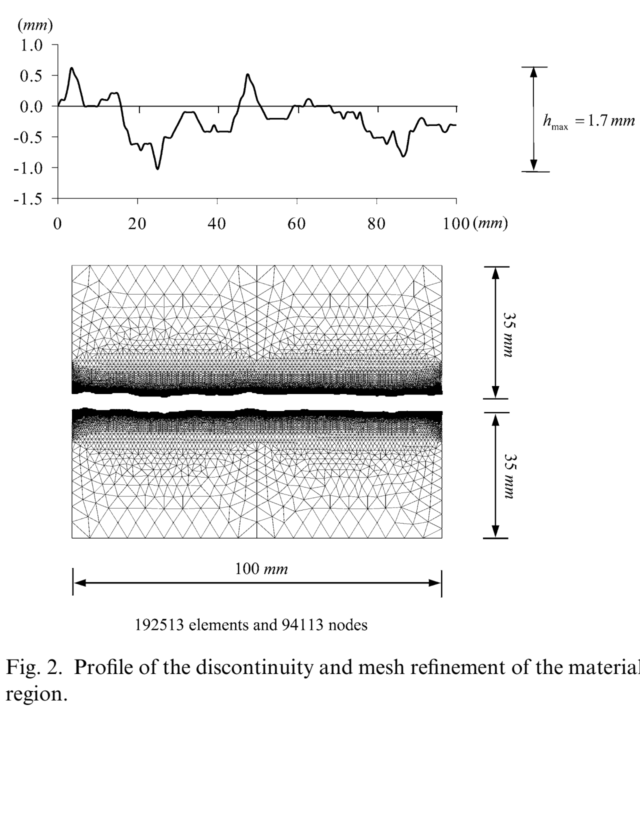

Fig. 2. Profile of the discontinuity and mesh refinement of the material region.

surface of the discontinuity has been determined through profiling techniques. This profile is used to develop the finite element discretization of the discontinuity. The basic question relates to the degree of mesh refinement that must be incorporated to faithfully reproduce the surface profile. There is no unique answer to this question. One can continue mesh refinement in the vicinity of the discontinuity to reflect the accuracy of the surface profiling technique, which in current day experimentation involving laser profiling can be as fine as a nanometer. Obviously, there are sensible limits that must be adopted by considering basic notions of the realm of applicability of the continuum concepts. For example, it would not be prudent to adopt a mesh refinement, which can accommodate a fraction of the grain size of the material that is being tested. In this case the computational estimates will most likely reflect the processes in the scale of the grains. Modelling of the overall shear behaviour of the joint in terms of continuum measures such as stresses in the contact regions, is best reflected by limiting the maximum size of elements to accommodate an assemblage of grains which will make the calculation of stresses both meaningful and computationally efficient. Admittedly, there is arbitrariness associated with the discretization of the surface profile and for this reason, different discretizations of surface refinement have been used. An example of a typical finite element discretization is shown in Fig. 2.

2.2. Constitutive modelling

The constitutive modelling of the problem should address several aspects including the non-linear behaviour of parent material and the frictional behaviour of the interface. The non-linear material models that are applicable to brittle geomaterials such as rocks and concrete are varied and quite numerous (see e.g., Chen [94], Chen and Saleeb [95], Desai and Siriwardane [96], Pande et al. [97], Darve [98], Pietruszczak and Pande [99], Davis and Selvadurai [100]) and from the point of view of the computational modelling exercise, attention is restricted to a conventional elastic- perfectly plastic model which is characterized by the additive decomposition of the incremental strain according to

$$\mathrm{d}\varepsilon_{ij} = \mathrm{d}\varepsilon_{ij}^{\mathrm{e}} + \mathrm{d}\varepsilon_{ij}^{\mathrm{p}}, \tag{1}$$

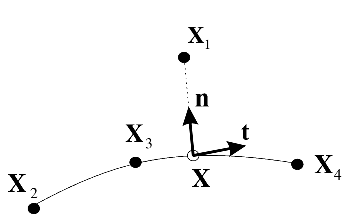

Fig. 3. A potential contact between a node and a line segment.

where the superscripts e and p refer to the elastic and plastic strain components, respectively. We define the incremental elastic strains through Hooke's law

$$\mathrm{d}\varepsilon_{ij}^{\mathrm{e}} = \frac{\mathrm{d}\sigma_{ij}}{2\mu} - \frac{\lambda\,\mathrm{d}\sigma_{kk}\delta_{ij}}{2\mu(3\lambda+2\mu)}, \tag{2}$$

where λ and μ are Lamé's constants (Davis and Selvadurai [101]). The plastic strain increments are defined through an associated flow rule of the form

$$\mathrm{d}\varepsilon_{ij}^{\mathrm{p}} = \mathrm{d}\xi\frac{\partial F}{\partial\sigma_{ij}}, \tag{3}$$

where $\mathrm{d}\xi$ is the plastic multiplier and $F(\sigma_{ij})$ is the yield function. In this study, the yield function is selected as the extended form of the Drucker–Prager yield condition defined by

$$F(\sigma_{ij}) = \sqrt{l_0^2 + 3J_2} + \frac{1}{3}I_1\tan\beta - d^*, \tag{4}$$

where

$$\tan\beta = \frac{3\sin\phi}{\sqrt{3+\sin^2\phi}}; \quad d^* = \frac{3c\cos\phi}{\sqrt{3+\sin^2\phi}}, \tag{5}$$

$$l_0 = d^* - \frac{f_{\mathrm{t}}}{3}\tan\beta; \quad c = \sqrt{\frac{f_{\mathrm{c}}f_{\mathrm{t}}}{2}} \tag{6}$$

and c, ϕ, f_{c} and f_{t} are the cohesion, the angle of friction, compressive strength and the tensile strength of the geomaterial. Also in (4), I_1 and J_2 are, respectively, the first invariant of the stress tensor and the second invariant of the stress deviator tensor. It should be borne in mind that these constitutive responses are not intended to exactly duplicate the geomaterial behaviour of the rock

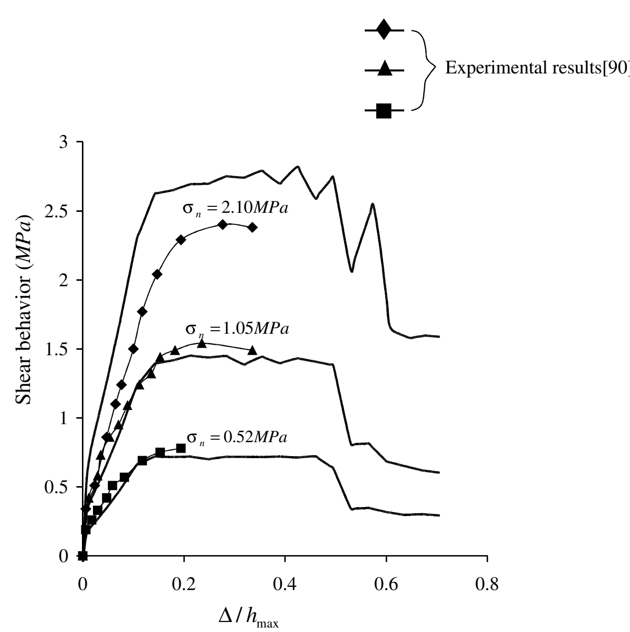

Fig. 4. Correlation with experimental data.

samples that were tested by Bandis et al. [92] but merely a plausible set of constitutive responses characteristic of brittle geomaterials that exhibit phenomenological plasticity phenomena. Also, with most brittle geomaterials of the type described by these relationships, the material parameters characterizing the plasticity model are effectively the three independent material constants β, f_c and f_t, the latter two parameters being identified with the more familiar values of uniaxial compressive and tensile strengths. The constitutive modelling of contact interaction is defined through a Coulomb friction model, which also accounts for certain *contact elasticity* prior to slip. The Coulomb friction response accounts only for the frictional shear stress response, and defined through the relative tangential slip Δ_s and shear stress τ. The relationship between the contact shear stress vs. relative shear deformation takes the form

$$\tau = k_s \Delta_s \quad \text{for} \quad \tau < \mu^* \sigma^*, \tag{7}$$

where Δ_s is the relative elastic tangential slip, σ^* is the local normal stress on the contact plane and $k_s = \mu^* \sigma^* / \gamma_{crit}$; once μ^* and γ_{crit} are specified and the local value of σ^* is computed, k_s is known. When $\tau \geqslant \mu^* \sigma^*$, slip occurs; prior to that, the relative movement between the surfaces occurs through a relative elastic tangential slip.

2.3. Incompatible deformations

The computational implementation of the elasto-plastic deformations and the associated Coulomb frictional phenomena are now considered to be relatively routine. The background information contained in the documentation for the ABAQUS finite element code is quite comprehensive and will not be repeated here. It is important to note an aspect of the computational methodologies that account for the development of incompatible movements at the discontinuity. This feature implies that the *initially-mated* surfaces of the discontinuity can experience finite differential movements in two directions but maintain contacts at locations that are newly formed as a result of the global differential movements. The ABAQUS code adopts a finite sliding computational algorithm to account for separation and sliding of finite amplitude and arbitrary rotation of the surfaces of contact (note that, although the external rotations of the regions composing the discontinuity are suppressed, the facility is there for development of element rotation at the local level).

2.4. Finite-sliding interaction

The two-dimensional contact between the two deformable surfaces has been modelled by finite-sliding interaction provided in the ABAQUS/Standard software [102]. Such algorithm adopts concept of the master and slave surfaces, which are defined to be in contact with

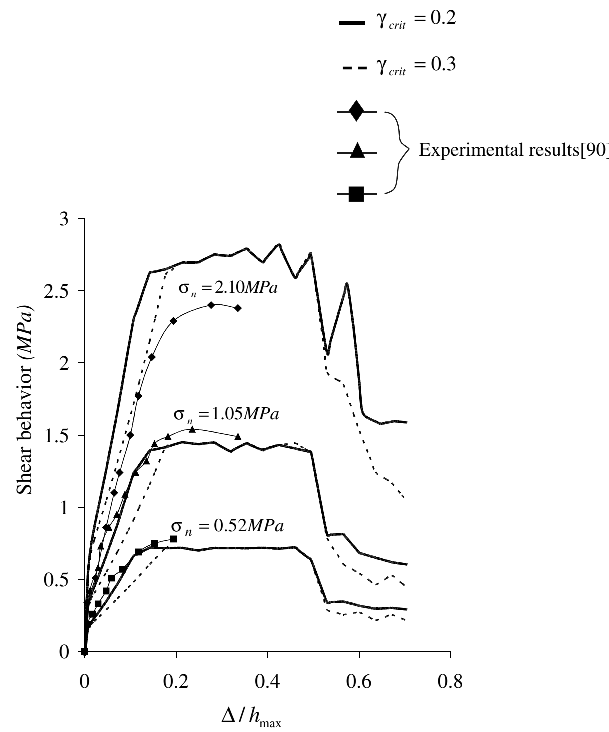

Fig. 5. Shear response at different γ_{crit}, μ^* = 0.6745.

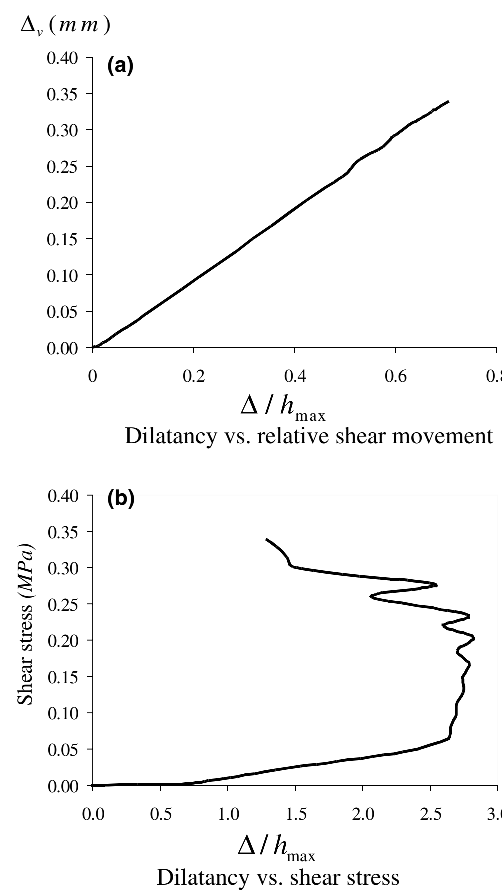

Fig. 6. Dilatancy during relative shearing (σ_n = 2.10 MPa, μ^* = 0.6745, γ_{crit} = 0.2).

each other. Consider contact of a node $\mathbf{X}_1$ on the slave surface with a segment of the master surface described by nodes $\mathbf{X}_2$, $\mathbf{X}_3$ and $\mathbf{X}_4$ (see Fig. 3). The potential contact point with $\mathbf{X}_1$ on the segment will be $\mathbf{X}$ such that $\mathbf{X}-\mathbf{X}_1$ will be normal to the local tangential to the segment described by nodes $\mathbf{X}_2$, $\mathbf{X}_3$ and $\mathbf{X}_4$. If we denote the unit normal and tangential vectors of the segment as $\mathbf{n}$ and $\mathbf{t}$, respectively, the vector of $\mathbf{X}-\mathbf{X}_1$ can be expressed as

$$\begin{aligned} &\mathbf{X}-\mathbf{X}_1=\mathbf{n}h, \\ &\mathbf{t}\cdot\mathbf{n}=0, \end{aligned} \tag{8}$$

where h is the distance between $\mathbf{X}_1$ and $\mathbf{X}$. At the same time, since $\mathbf{X}$ is located on the segment, its position then can be interpolated by nodes $\mathbf{X}_2$, $\mathbf{X}_3$ and $\mathbf{X}_4$, through

$$\mathbf{X}=\sum_{i=2}^{4} N_i(g)\mathbf{X}_i, \tag{9}$$

where N_i (i = 2, 3, 4) are the interpolation functions of a variable g. By using Eq. (8), the vector $\mathbf{n}h$ can be expressed by another set of interpolating functions $\overline{N}_i$ $(i=1,2,3,4)$

$$\mathbf{n}h=\sum_{i=1}^{4}\overline{N}_i(g)\mathbf{X}_i, \tag{10}$$

where

$$\begin{aligned} &\overline{N}_1(g)=-1, \\ &\overline{N}_i(g)=N_i(g) \quad (i=2,3,4). \end{aligned} \tag{11}$$

The tangential vector $\mathbf{t}$ can be written as

$$\mathbf{t}=\frac{\mathrm{d}\mathbf{X}}{\mathrm{d}g}\bigg/\left|\frac{\mathrm{d}\mathbf{X}}{\mathrm{d}g}\right|=\frac{\mathrm{d}\mathbf{X}}{\mathrm{d}s}=\frac{\sum_{i=2}^{4}\mathrm{d}N_i\mathbf{X}_i}{\mathrm{d}s}=\frac{\sum_{i=1}^{4}\mathrm{d}\overline{N}_i\mathbf{X}_i}{\mathrm{d}s}. \tag{12}$$

The linearization of (10) gives

$$\begin{aligned} \delta\mathbf{n}h+\mathbf{n}\delta h &=\sum_{i=1}^{4}(\delta\overline{N}_i\mathbf{X}_i+\overline{N}_i\delta\mathbf{X}_i) \\ &=\mathbf{t}\delta s+\sum_{i=1}^{4}\overline{N}_i\delta\mathbf{X}_i. \end{aligned} \tag{13}$$

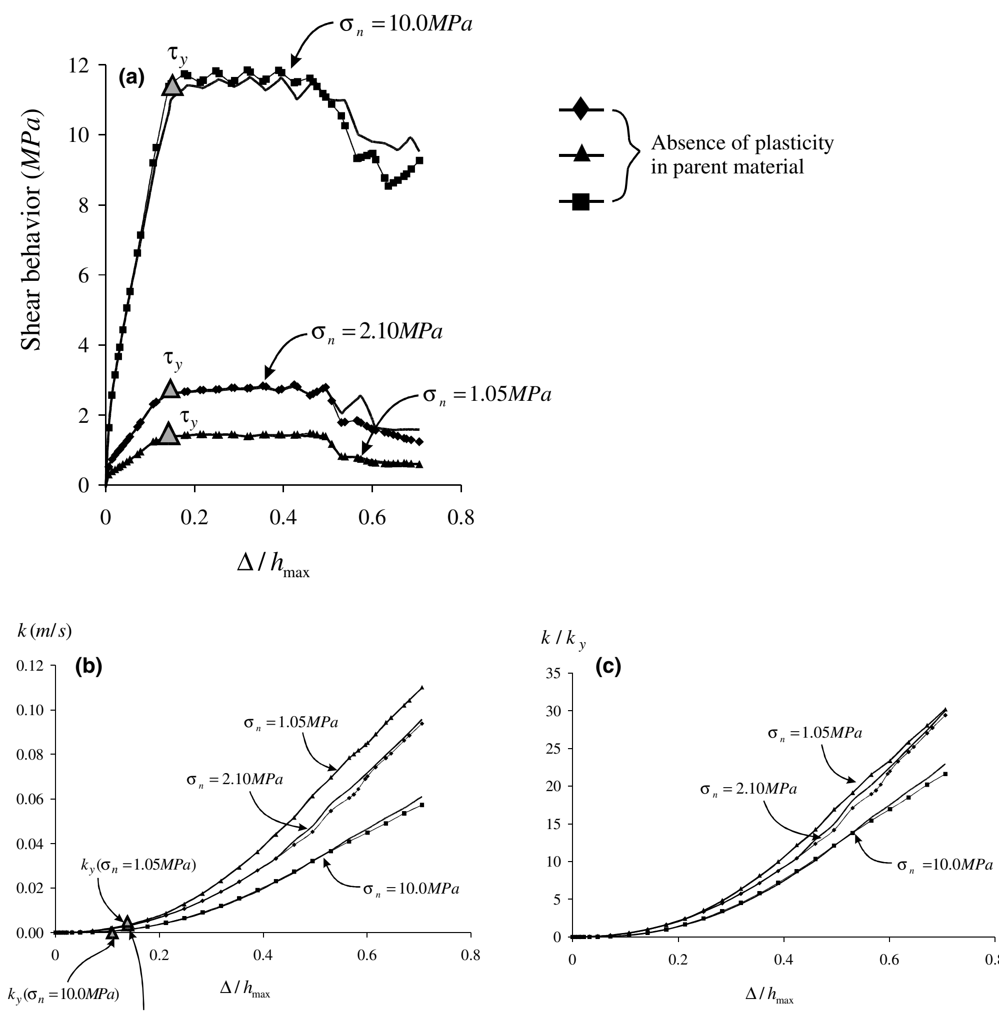

Fig. 7. Comparison of shear behavior of the discontinuity. Influence of geomaterial plasticity (γ_{crit} = 0.2 and μ^* = 0.6745).

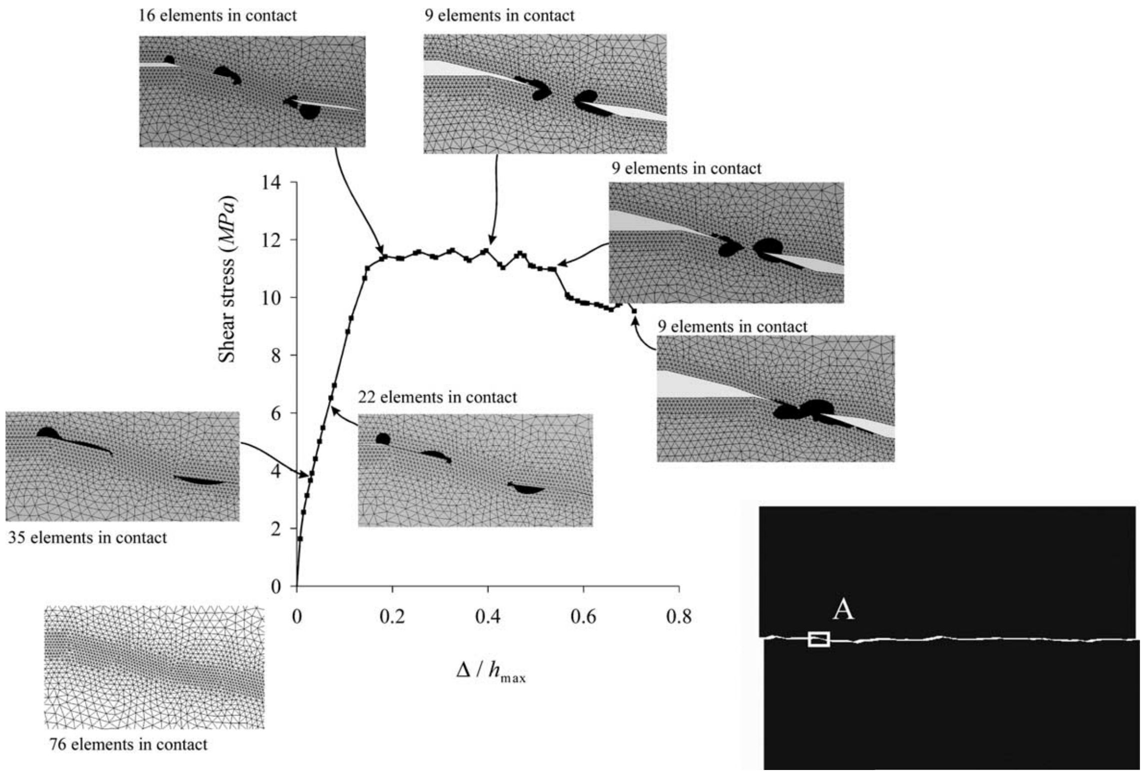

Fig. 8. Discontinuous movements and plasticity generation at contact location 'A' (σ_n = 10.0 MPa, γ_{crit} = 0.2 and μ^* = 0.6745).

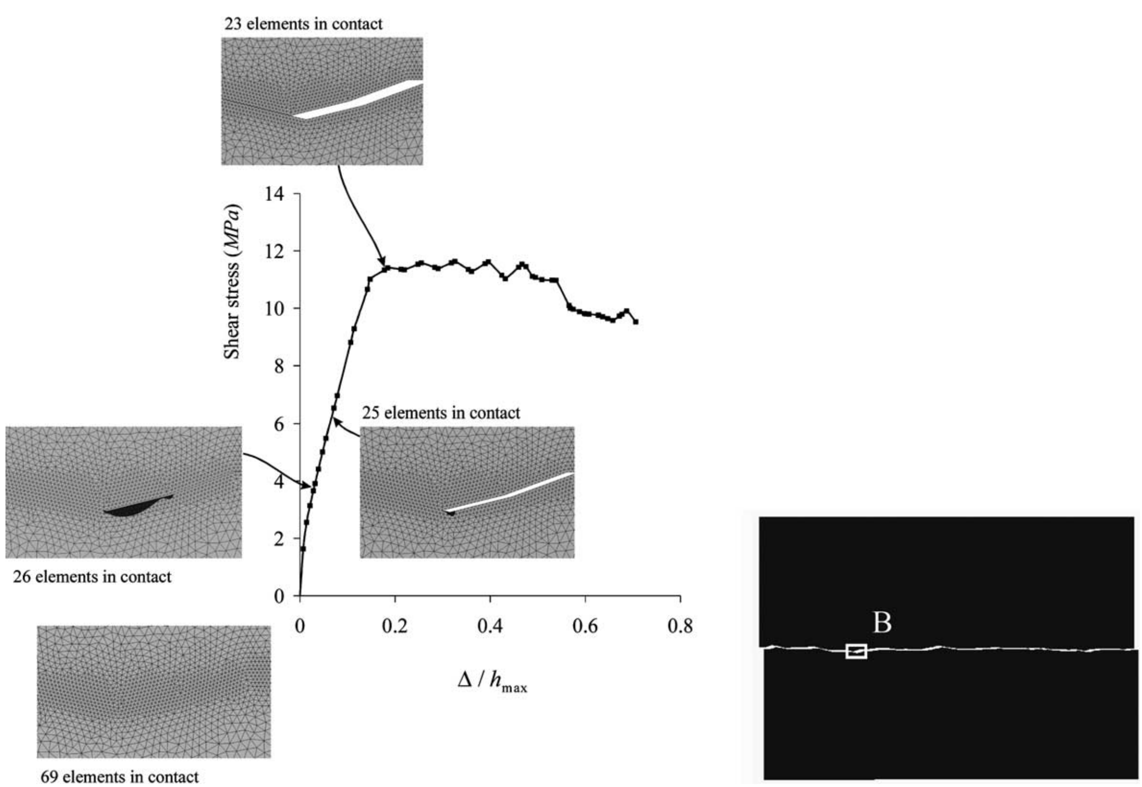

Fig. 9. Discontinuous movements and plasticity generation at contact location 'B' (σ_n = 10.0 MPa, γ_{crit} = 0.2 and μ^* = 0.6745).

In the direction of **n** and **t**, (13) yields

$$\delta h = \sum_{i=1}^{4} \overline{N}_i \mathbf{n} \cdot \delta \mathbf{X}_i, \qquad \delta s = -\sum_{i=1}^{4} \overline{N}_i \mathbf{t} \cdot \delta \mathbf{X}_i - h\mathbf{t} \cdot \delta \mathbf{n}, \tag{14}$$

where δs is defined as a slip, and it is only relevant when $\mathbf{X}_1$ is on the segment where $h = 0$. From this, we obtain

$$\delta h = \sum_{i=1}^{4} \overline{N}_i \mathbf{n} \cdot \delta \mathbf{X}_i, \qquad \delta s = -\sum_{i=1}^{4} \overline{N}_i \mathbf{t} \cdot \delta \mathbf{X}_i. \tag{15}$$

The second variations of h and s can be similarly calculated as

$$\mathrm{d}\delta h = -\sum_{i=1}^{4}\sum_{j=1}^{4} \delta \mathbf{X}_i \cdot \left(\mathbf{n}\frac{\mathrm{d}\overline{N}_i}{\mathrm{d}s}\overline{N}_j \mathbf{t} + \mathbf{t}\overline{N}_i \frac{\mathrm{d}\overline{N}_j}{\mathrm{d}s}\mathbf{n} + \mathbf{t}\overline{N}_i \rho_n \overline{N}_j \mathbf{t} \right) \cdot \mathrm{d}\mathbf{X}_j,$$
$$\mathrm{d}\delta s = \sum_{i=1}^{4}\sum_{j=1}^{4} \delta \mathbf{X}_i \cdot \left(\mathbf{t}\frac{\mathrm{d}\overline{N}_i}{\mathrm{d}s}\overline{N}_j \mathbf{t} - \mathbf{n}\overline{N}_i \frac{\mathrm{d}\overline{N}_j}{\mathrm{d}s}\mathbf{n} - \mathbf{n}\overline{N}_i \rho_n \overline{N}_j \mathbf{t} \right) \cdot \mathrm{d}\mathbf{X}_j, \tag{16}$$

where

$$\rho_n = -\mathbf{n} \cdot \frac{\mathrm{d}^2\mathbf{X}}{\mathrm{d}g^2} \bigg/ \left|\frac{\mathrm{d}^2\mathbf{X}}{\mathrm{d}g^2}\right|^2. \tag{17}$$

The details of the derivations are given in the documentation of the ABAQUS code [102]. The formulation of the first and second variations of h and s are useful in constructing the stiffness matrix in the non-linear finite element algorithm (see Bathe [103], Zienkiewicz and Taylor [104], El-Abbasi and Bathe [105], Wriggers and Wagner [106] and Willner [107]).

3. Computational simulations

We now examine the mechanical behaviour of a typical discontinuity in a brittle geomaterial taking into consideration the three aspects of the study, namely, the fine structure of the discontinuity simulated at a scale consistent with the structure of the material and the capabilities of the computational facilities, the elastic–plastic phenomena in the parent material composing the discontinuity, the frictional phenomena at the contacting surfaces and the influence of incompatible deformations at the initially-mated surfaces. Since an objective of the study is also to develop certain plausible simulations of the experiments conducted by Bandis et al. [92], the profile of the discontinuity is matched as closely as possible with the "joint profile" provided in that study. The element discretization involves 192513 six-noded triangular elements and 94113 nodes. The Fig. 2 illustrates the finite element discretization of the initially mated surfaces of the discontinuity. The

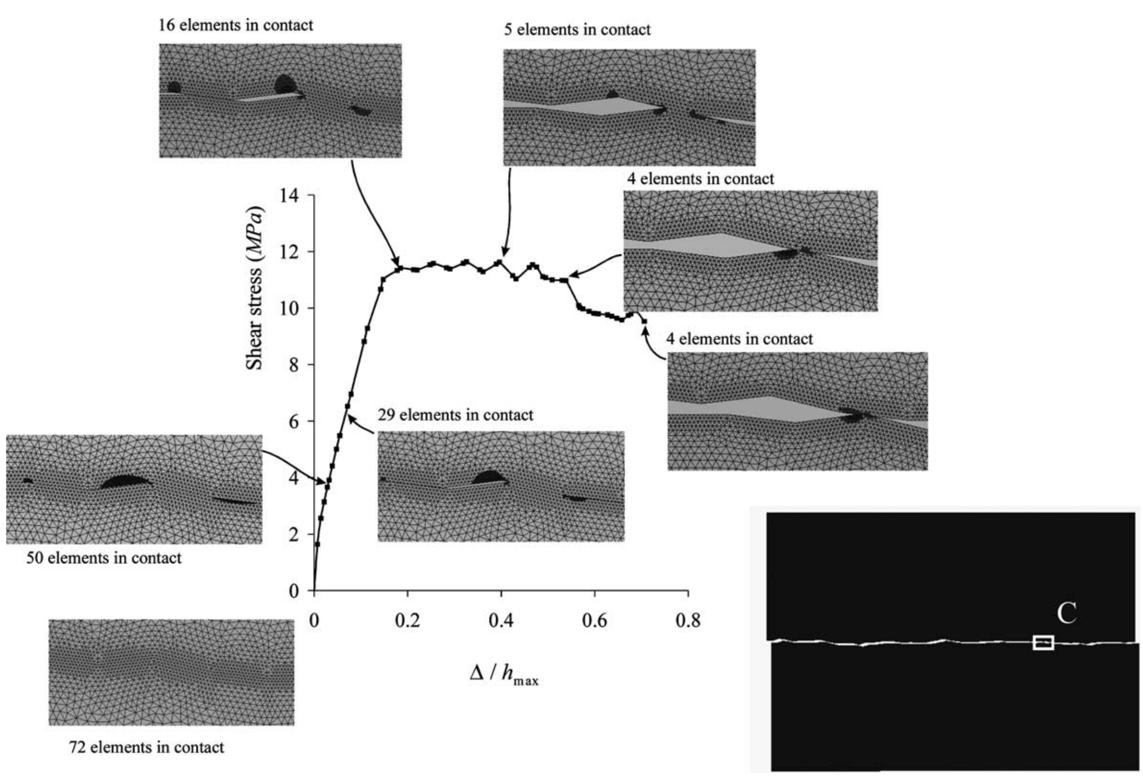

Fig. 10. Discontinuous movements and plasticity generation at contact location 'C' (σ_n = 10.0 MPa, γ_{crit} = 0.2 and μ^* = 0.6745).

surfaces are shown separated to highlight the irregular profile. The overall length of the discontinuity is 100 mm and the maximum asperity difference is $h_{\max} = 1.7$ mm. The smallest dimension of an element at the discontinuity itself is 0.05 mm.

The constitutive modelling of the parent material region requires the specification of the isotropic elastic constants and three strength parameters. These are representative of "dolerite-type" rocks that have been used in the investigations (Jaeger and Cook [108]). The numerical values of the parameters are as follows:

$$f_c \approx 160 \text{ MPa};\quad f_t \approx 17 \text{ MPa};\quad \beta \approx 52^\circ,\\ E \approx 78 \text{ GPa};\quad v \approx 0.23. \tag{18}$$

The friction angle for the discontinuity quoted by Bandis et al. [92] is 34°, which corresponds to a coefficient of friction of $\mu^* \approx 0.6745$; whereas in the literature, the cited values give $\mu^* \in (0.64, 0.90)$. The remaining parameter relates to γ_{crit}, which governs the maximum elastic slip at the contact. The parameter γ_{crit} that governs the maximum elastic slip is not one that is determined in any conventional experimentation. As such, this parameter either has to be back calculated or assigned a plausible range consistent with data available in the literature. In this study, the parameter γ_{crit} is chosen to match with a limited data set for the shear stress vs. relative shear displacement (say, at the lowest global

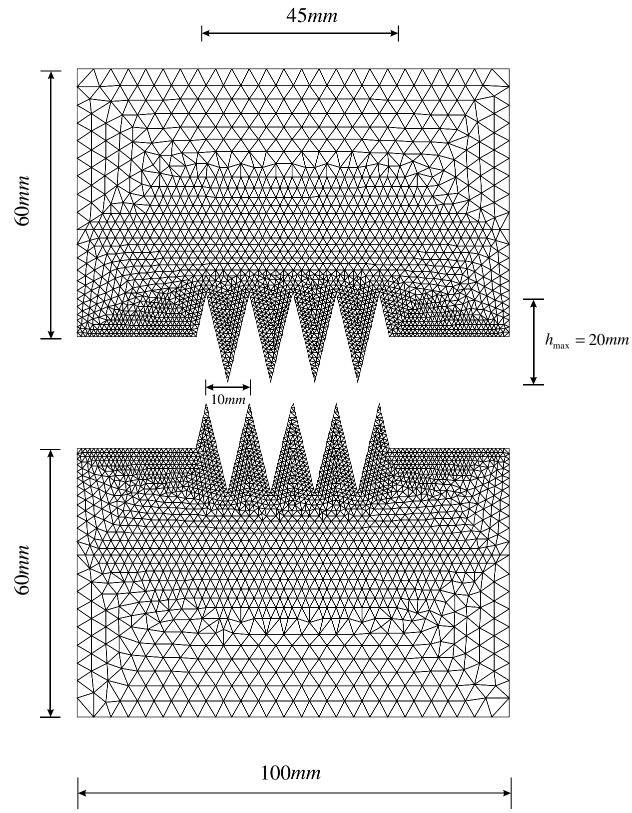

Fig. 12. Mesh configuration of an idealized discontinuity.

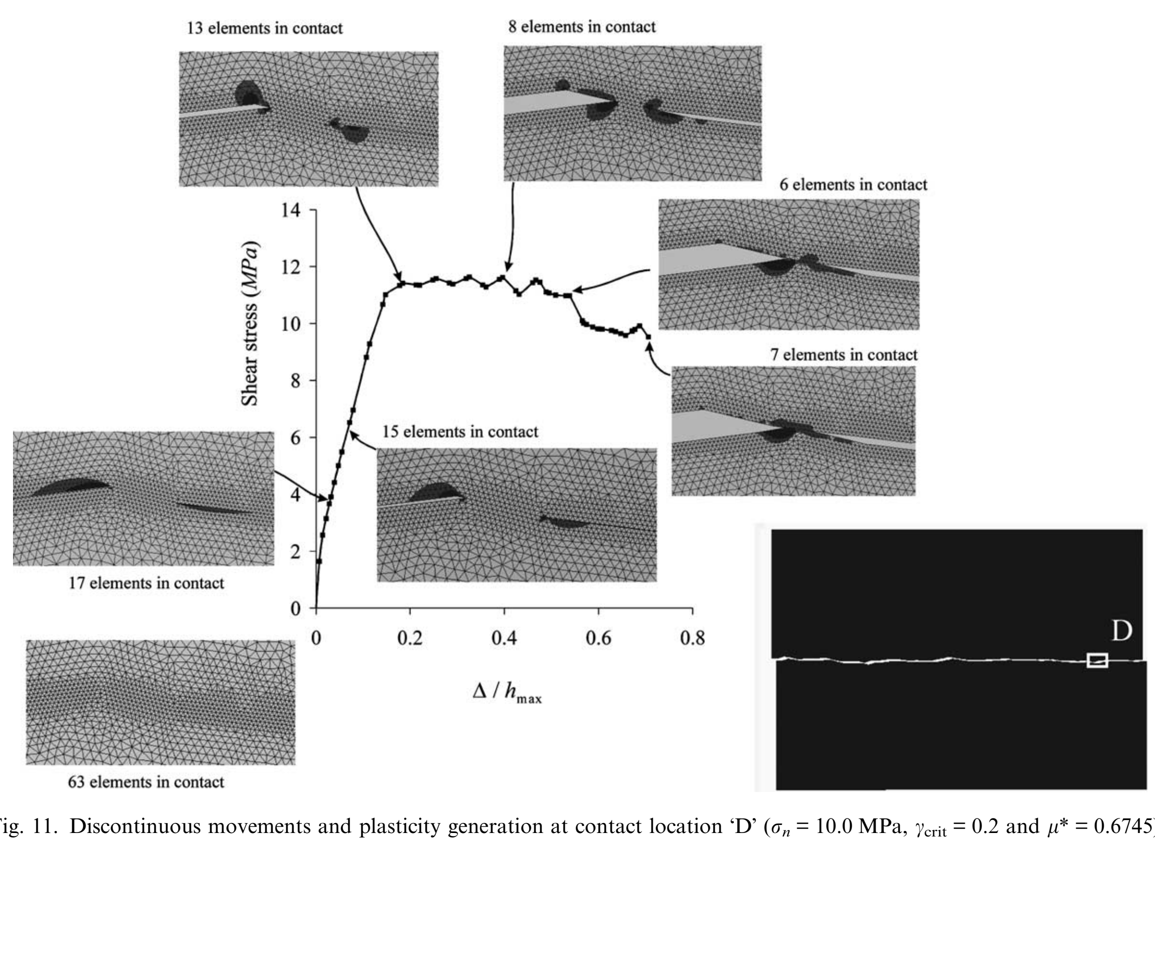

Fig. 11. Discontinuous movements and plasticity generation at contact location 'D' ($\sigma_n = 10.0$ MPa, $\gamma_{\text{crit}} = 0.2$ and $\mu^* = 0.6745$).

normal stress applied to the discontinuity) and computational predictions are then made for other levels of the normal stress. The sensitivity study is also conducted by altering the parameter γ_{crit}, to either *one half* or *double* the value obtained by matching the computational and experimental data sets.

Figs. 4 and 5 illustrate the comparisons between the experimental results for the shear stress vs. relative shear displacement obtained by Bandis et al. [92] for the dolerite joint and the computational results obtained via the modelling procedure described previously. The relative shear movement is normalized with respect to the geometry of the profile of the discontinuity as defined by h_{max}. The experiments involve three levels of the normal stress that is applied to the joint (0.52 MPa, 1.05 MPa and 2.10 MPa). The experimental results are calibrated, at the lowest applied normal stress, to determine the parameter γ_{crit} governing critical elastic slip, and this value is kept constant in the subsequent computational evaluations. The computational procedure is then repeated by setting the value of γ_{crit} at 0.30, to ascertain the sensitivity of the parameter to the computational evaluations. An important aspect to observe in studies of this nature relates not to the specific values, but rather to trends of the computational estimates. The results of these preliminary calculations indicate that the *trends* in the global shear response of the discontinuity can be duplicated through the computational simulations. This research investigation also focuses on the assessment of the contributions of plasticity phenomena in the parent rock on the shear behaviour under constant normal stress. Attention is now focused on the evaluation of the dilatancy of the discontinuity associated with relative shear. Fig. 6 illustrates the evolution of dilatancy of the joint as a function of the relative shear, for the case involving the largest level of applied normal loading. The dilatancy of the discontinuity is calculated in terms of the average discontinuity opening movement Δ_v. Fig. 7(a) and (b) illustrates the shear and dilatancy behaviour of the discontinuity either in the presence or absence of material plasticity. Since joint profile is comparatively flat, the influence of the presence

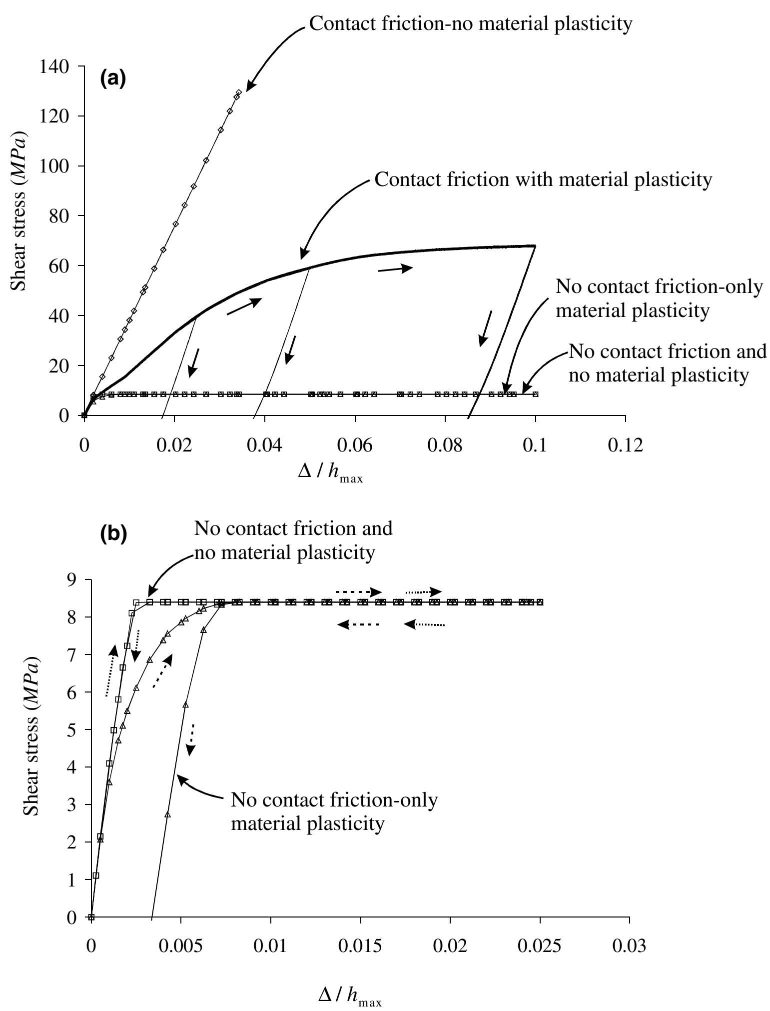

Fig. 13. Comparison of shear behavior of an idealized discontinuity. Influence of geomaterial plasticity (σ_n = 2.10 MPa, γ_{crit} = 0.2 and μ^* = 0.6745).

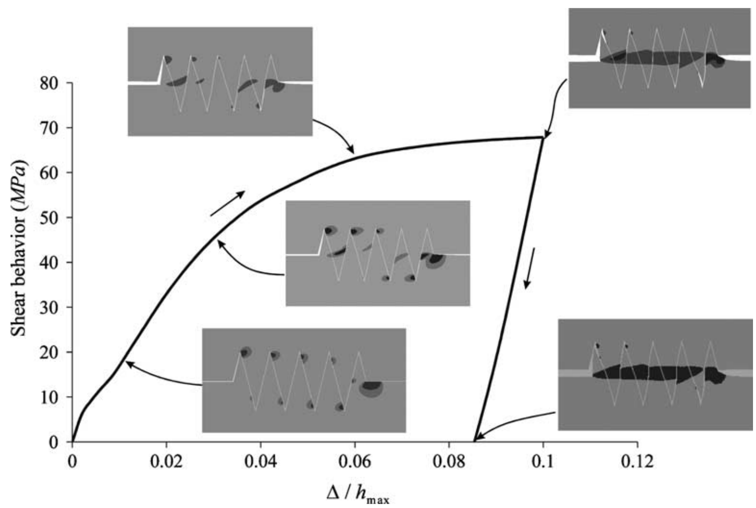

Fig. 14. Discontinuous movements and plasticity generation during shearing of an idealized joint (σ_n = 2.10 MPa, γ_{crit} = 0.2 and μ^* = 0.6745).

of plasticity is not noticeable at low normal stresses; the computational evaluations are then conducted at a higher normal stress of 10 MPa. At this normal stress, the influence of parent material plasticity is noticeable particularly at large shear displacements (e.g., $\Delta/h_{max} = 0.5–0.7$). The evolution of dilatancy can be viewed as the evolution of hydraulic conductivity of the discontinuity in a direction normal to the direction of shear. The dilatancy-induced overall increase in the volume of the initially-mated discontinuity can be interpreted through an elementary parallel plate or Hele–Shaw model (Snow [66], Boulon et al. [80], and Selvadurai [109]) for the flow of a viscous fluid through a narrow aperture. The hydraulic conductivity of the discontinuity experiencing shear-induced dilatancy is then given by the classical relationship

$$k = \frac{(\Delta_v)^2 \rho g}{12\eta}, \tag{19}$$

where η is the dynamic shear viscosity of the permeating fluid and ρ is its mass density. Fig. 7(b) shows the variation of the hydraulic conductivity of the dilating discontinuity as a function of the normalized discontinuous shear movement, and calculated for typical values of the dynamic shear viscosity and density of water at room temperature ($\eta = 1.0 \times 10^{-3}$ kg/ms; $\rho = 998$ kg/m^3 at room temperature 21 °C). The non-dimensional estimate given in Fig. 7(c) normalizes the variations of hydraulic conductivity with respect to the value of the hydraulic conductivity evaluated at the transition of the shear stress τ_y from a monotonically increasing curve to a plateau. Figs. 8–11 also illustrates the discontinuous movement pattern that contributes to the development of dilatancy, and the zones in which plastic flow takes place in the regions adjacent to the discontinuity. In order to illustrate the generation of plasticity more effectively, the computation are performed for a case where normal stress is 10 MPa. In region A, C and D, the effects of plasticity become more pronounced and the number of elements in contact reduces as relative shear increases. In region B, while plastic flow in the material region is observed at the initial stages of shearing, these effects become less pronounced as the relative shear increases. It should be noted that the inset Figures are relevant to only a small segment of the discontinuity indicated by the highlighted regions.

As a conclusion, to examine the effects of the joint friction and parent material plasticity on the mechanical behavior of the discontinuity, we examine the problem of an idealized discontinuity with maximum asperity height difference of h_{max} = 20.0 mm over a 45 mm region (see Fig. 12). The boundary conditions are the same as those for natural joint examined previously. The normal stress is set as σ_n = 2.10 MPa . The mesh configuration used in the computation is presented in Fig. 12. The smallest dimension of an element in the discretization is 1 mm . The material properties are chosen to be as the same as those for the natural joint. Comparisons for the shear response of the discontinuity in the presence and absence of parent material plasticity are indicated in Fig. 13. The presence of plasticity in parent material has significant influence on the shear behavior of the idealized discontinuity. The development of the plastic zones in the parent material surrounding discontinuity is shown in Fig. 14. The computations predict the plastic yielding of the asperities at the attainment of the peak shear capacity.

4. Concluding remarks

The computational modelling of the mechanical behaviour of a discontinuity is a useful exercise for purposes of identifying factors and processes that can influence its shear behaviour. Such modelling can take into consideration features of the profile, frictional effects at the contacting plane, non-linear phenomena in the parent material and incompatible movements at the contacting planes of the discontinuity. As an example, the computational approach is applied to model the experimental study of a discontinuity in a dolerite sample that has been reported in the literature. The computational methodology adopted also accounts for certain sensitivity analysis to account for parameters that are not reported in experimental data and not readily available in the literature. The computational results show that the overall *experimental trends* in the shear behaviour of the discontinuity can be duplicated reasonably accurately through the computational scheme. The study also presents a preliminary assessment of the influence of parent material plasticity on the shear behaviour of the discontinuity. The preliminary results indicate that the influence of plasticity of the parent material becomes important only at values of relative shear movement comparable to the maximum value of the differential height of the profile of the discontinuity. The computational scheme also predicts the evolution of dilatant movement of the discontinuity with increasing shear displacement. This information can be used to estimate the evolution of hydraulic conductivity of the discontinuity in a direction orthogonal to the direction of shear displacement.

References

[1] Coulomb CA. Théorie des machines simples. Mémoire de mathématique et Physique de l'Académie Royale 1785;10:161–342.

[2] Bowden FP, Tabor D. The friction and lubrication of solids. Oxford: Clarendon Press; 1986.

[3] Johnson KL. Contact mechanics. Cambridge: Cambridge University Press; 1985.

[4] Patton FD. Multiple modes of shear failure in rock. In: Proceedings of the 1st congress of ISRM, vol. 1. Laboratório nacional de engenharia civil, Lisboa; 1996. p. 509–13.

[5] Ladanyi B, Archambault G. Shear strength and deformability of filled indented joints. In: International symposium: the geotechnics of structurally complex formations, Capri; 1977. p. 371–26.

[6] Barton NR. A relationship between joint roughness and joint shear strength. In: Rock fracture: Proceedings of the international symposium on rock mechanics, Nancy, France; 1971. p. 1–8.

[7] Barton NR, Choubey V. The shear strength of rock joints in theory and practice. Rock Mech 1977;10:1–54.

[8] International Society for Rock Mechanics. Commission on Standardization of Laboratory and Field Tests, Suggested methods for the quantitative description of discontinuities in rock masses. Int Rock Mech Min Sci Geomech Abstr 1978;15:319–68.

[9] Tse R, Cruden DM. Estimating joint roughness coefficients. Int Rock Mech Min Sci Geomech Abstr 1979;16:303–7.

[10] Reeves MJ. Rock surface roughness and frictional strength. Int Rock Mech Min Sci Geomech Abstr 1985;22:429–42.

[11] Lee YH, Carr JR, Barr DJ, Haas CJ. The fractal dimension as a measure of the roughness of rock discontinuity profile. Int Rock Mech Min Sci Geomech Abstr 1990;27:453–64.

[12] Xie H, Wang JA, Xie WH. Fractal effects of surfaces roughness on the mechanical behavior of rock joints. Chaos Soliton Fract 1997;8:221–52.

[13] Huang TH, Doong YS. Anisotropic shear strength of rock joints. In: Rock joints: Proceedings of the international symposium on rock joints, Loen, Norway; 1990. p. 211–8.

[14] Jing L, Nordlund E, Stephansson O. An experimental study on the anisotropy and stress-dependency of the strength and deformability of rock joints. Int J Rock Mech Min Sci Geomech Abstr 1992;29:535–42.

[15] Seidel JP, Haberfield CM. The use of fractal geometry in a joint shear model. In: Mechanics of jointed and faulted rock: Proceedings of the 2nd international conference on mechanics of jointed and faulted rock, MJFR-2, Vienna, Austria; 1995. p. 529–34.

[16] Grasselli G, Egger P. 3D. Surface characterization for the prediction of the shear strength of rough joints. Eurock 2000, Aachen 2000:281–6.

[17] Brown SR, Scholz CII. Broad band width study of the topography of natural rock surfaces. J Geophys Res 1985;90:12575–82.

[18] Turk N, Grieg MJ, Dearman WR, Amin FF. Characteriztion of rock joint surfaces by fractal dimension. In: Rock mechanics: Proceedings of the 28th US symposium; 1987. p. 1223–36.

[19] Carr JR. Rock mass classification using fractal dimension. In: Proceedings of the 28th US Symposium on rock mechanics, Tucson; 1987. p. 73–80.

[20] Wakabayashi N, Fukushige I. Experimental study on the relation between fractal dimension and shear strength. In: Mechanics of jointed and faulted rock, Proceedings of the 2nd international conference, MJFR-2, Vienna; 1995. p. 119–24.

[21] Xie H, Pariseau WG. Fractal estimation of joint roughness coefficients. Science in China (Series B) 1994;34:1516–24.

[22] Gentier S, Riss J, Archambault G, Flamand R, Hopkins D. Influence of fracture geometry on shear behavior. Int Rock Mech Min Sci 2000;37:161–74.

[23] Davis RO, Salt G. Strength of undulating shear surfaces in rock. Geotechnique 1986;36:503–9.

[24] Kodikara JK, Johnston IW. Shear behaviour of irregular triangular rock-concrete joints. Int J Rock Mech Min Sci Geomech Abstr 1994;31:313–22.

[25] Armand G, Boulon MJ, Papadopoulos C, Basanou ME, Vardoulakis IP. Mechanical behaviour of Dionysos marble smooth joints: I. Experiments. In: Mechanics of jointed and faulted rock: Proceedings of the 3rd international conference, MJFR-3, Vienna; 1998. p. 159–64.

[26] Armand G, Boulon MJ, Hoteit N, Cannic S. Mechanical behaviour of natural joints of granodiorite under high normal stress. In: Mechanics of jointed and faulted rock. Proceedings of the third international conference, MJFR-3, Vienna; 1998. p. 217–22.

[27] Yang ZY, Chiang DY. An experimental study on the progressive shear behaviour of rock joints with tooth-shaped asperities. Int Rock Mech Min Sci Geomech Abstr 2000;37:1247–59.

[28] Brekke TL. On the measurement of the relative potential swellability of hydrothermal montmorillonite clay from joints and faults in the Pre-Cambrian and Paleozoic rocks in Norway. Int Rock Mech Min Sci Geomech Abst 1965;2:155–65.

[29] Brekke TL, Selmer-Olsen R. Stability problems in underground constructions caused by montmorillonite-carrying joints and faults. Eng Geol 1965;1:3–19.

[30] Bernaix J. Etude géotechnique de la roche de Malpasset. Paris: Dunod; 1967.

[31] Romero SV. In situ direct shear on irregular-surface joints filled with clayey material. ISRM Rock Mech Symp, Madrid 1968;1:189–94.
[32] Schnitter NJ, Schneider TR. Abutment stability investigations for Emossen arch dam. In: Proceedings of the 10th international congress on large dams, Montreal, vol. 2; 1970. p. 69–87.
[33] Goodman RE. The deformability of joints. ASTM: Special Tech Publ 1970:174–96.
[34] Tulinov R, Molokov L. Role of joint filling material in shear strength of rocks. In: Proceedings of the ISRM symposium, Nancy, France; 1971. Paper II-24.
[35] Goodman RE, Taylor RL, Brekke TL. A model for the mechanics of jointed rock. J Soil Mech Found Div Proc ASCE 1968;94:637–59.
[36] Zienkiewicz OC, Best B, Dullage C, Stagg KG. Analysis of nonlinear problems in rock mechanics with particular reference to jointed rock systems. In: Proceedings of the 2nd congress of international society for rock mechanics, Beograd, vol. 2; 1970. p. 501–9.
[37] Mahtab MA, Goodman RE. Three-dimensional finite element analysis of jointed rock slopes. In: Proceedings of the 2nd Congress, ISRM, Beograd, vol. 3; 1970. p. 7–22.
[38] Fredriksson G. Finite element simulation of surface non-linearities in structural mechanics. Comput Struct 1976;6:281–90.
[39] Ghaboussi J, Wilson EL, Isenberg J. Finite elements for rock joints and interfaces. J Soil Mech Fdn Div Proc ASCE 1973;99:833–48.
[40] Herrmann LR. Finite element analysis of contact problems. J Eng Mech Div Proc ASCE 1978;104:1042–57.
[41] Pande GN, Sharma KG. On joint/interface elements and associated problems of numerically ill-conditioning. Int J Num Anal Meth Geomech 1979;3:293–302.
[42] Katona MG. A simple contact–friction interface element with applications to buried culverts. Int J Num Anal Meth Geomech 1983;7:371–84.
[43] Selvadurai APS, Faruque MO. The influence of interface frictionon the performance of cable jacking tests of rock masses. In: Implementation of computer procedures and stress–strain laws in geotechnical engineering. Proc Symp, Chicago, vol. 1; 1981. p. 169–83.
[44] Desai CS. Behaviour of interfaces between structural and geologic media. In: Proceedings of the international conference on recent advances in geotech. Earthquake Engineering and Soil Dynamics, St. Louis, MO; 1981. p. 619–38.
[45] Desai CS, Zaman MM, Lightner JG, Siriwardane HJ. Thin-layer element for interfaces and joints. Int J Num Anal Meth Geomech 1984:19–43.
[46] Desai CS, Nagaraj BK. Modelling of normal and shear behaviour at contacts and interfaces. J Eng Mech Div Proc ASCE 1988;114:1042–57.
[47] Goodman RE, Dubois J. Duplication of dilatancy in analysis of jointed rocks. J Soil Mech Fdn Div Proc ASCE 1972;98:399–422.
[48] Heuze FE, Barbour TG. New models for rock joints and interfaces. J Geotech Eng Div Proc ASCE 1982;108:757–76.
[49] Leichnitz W. Mechanical properties of rock joints. Int J Rock Mech Min Sci Geomech Abstr 1985;22:313–21.
[50] Carol I, Gens A and Alonso EE. A three-dimensional elasto-plastic joint element. In: Proceedings of the international symposium on fundamentals of rock joints, 1985. p. 441–51.
[51] Gens A, Carol I, Alonso EE. Rock joints: FEM implementation and applications. In: Mechanics of geomaterial interfaces. New York: Elsevier; 1995. p. 395–420.
[52] Boulon MJ, Nova R. Modelling of soil-structure interface behaviour, a comparison between elastoplastic and rate-type law. Comput Geotech 1990;9:21–46.
[53] Aubry D, Modaressi A. A constitutive model for cyclic behaviour of interfaces with variable dilatancy. Comput Geotech 1990;9:47–58.
[54] Hohberg J-M. Concrete joints. In: Mechanics of geomaterial interfaces. New York: Elsevier; 1995. p. 421–46.
[55] Plesha ME. Constitutive models for rock discontinuities with dilatancy and surface degradation. Int J Numer Anal Meth Geomech 1987;11:345–62.
[56] Hutson RW, Dowding CH. Joint asperity degradation during cyclic shear. Int J Rock Mech Min Sci Geomech Abstr 1990;27:109–19.
[57] Plesha ME, Ballarini R, Parulekar A. Constitutive model and finite element procedure for dilatant contact problems. J Engng Mech Div Proc ASCE 1989;115:2649–68.
[58] Qiu X, Plesha ME, Haimson BC, Huang X. An investigation of the mechanics of rock joints. Int J Rock Mech Min Sci Geomech Abstr 1993;30:271–87.
[59] Nguyen TS, Selvadurai APS. A model for coupled mechanical and hydraulic behavior of a rock joint. Int J Numer Anal Meth Geomech 1998;22:29–48.
[60] Indraratne B, Haque A. Shear behaviour of rock joints. Rotterdam: A.A. Balkema; 2000.
[61] Andersson T. The boundary element method applied to two-dimensional contact problems with friction. In: Boundary element methods, Proceedings of the 3rd international seminar, Irvine, CA; 1981.
[62] Crotty JM, Wardle LJ. Boundary element analysis of piecewise homogeneous media with structural discontinuities. Int J Rock Mech Min Sci Geomech Abstr 1985;22:419–27.
[63] Selvadurai APS, Au MC. Boundary element modelling of interface phenomena. In: Topics in boundary element research. Berlin: Springer Verlag; 1987. p. 112–26. [Chapter 5].
[64] Selvadurai APS. The role of geomaterial interface degradation on the mechanics of a fracture. In: Mechanics of jointed and faulted rock: Proceedings of the 2nd international conference on mechanics of jointed and faulted rock, MJFR-2, Vienna; 1995. p. 1031–38.
[65] Beer G, Poulsen BA. Rock joints-BEM computations. In: Mechanics of geomaterial interfaces. New York: Elsevier; 1995. p. 343–73.
[66] Snow DT. A parallel plate model of fractured permeable media. PhD thesis, University of California, Berkeley; 1965.
[67] Brace WF. Note on permeability changes in geologic material due to stress. Pure Appl Geophys 1978;116:627–33.
[68] Kranz RL, Frankel AD, Engelder T, Scholz CH. The permeability of whole and jointed barre granite. Int Rock Mech Min Sci Geomech Abstr 1979;16:225–34.
[69] Raven KG, Gale JE. Water flow in a natural rock fracture as a function of the stress and sample size. Int Rock Mech Min Sci Geomech Abstr 1985;22:251–61.
[70] Walsh JB. Effect of pore pressure and confining pressure on fracture permeability. Int Rock Mech Min Sci Geomech Abstr 1981;18:429–35.
[71] Engelder T, Scholz CH. Fluid flow along a very smooth joints at effective pressure up to 200 megapascals. In: Mechanical behavior of crustal rocks. Washtington, DC: Amer Geophys Union Monograph; 1981.
[72] Gale JE. Assessing the permeability characteristics of fractured rock. Geol Soc Am, Special Paper 1982;189:163–80.
[73] Haimson BC, Doe TW. State of stress, permeability and fractures in the precambrian granite of Northern Illinois. J Geophys Res 1983;88:7355–71.
[74] Bandis SC, Makurat A, Vik G. Predicted and measured hydraulic conductivity of rock joints. In: Proceedings of the international symposium on fundamentals of rock joints, Bjorkliden; 1985. p. 269–80.

[75] Pyrak-Nolte LJ, Myer LR, Cook NGW, Witherspoon PA. Hydraulic and mechanical properties of natural joints in low permeability rock. In: Proceedings of the 6th international congress on rock mechanics, Montreal; 1987. p. 225–31.
[76] Teufel LW. Permeability changes during shear deformation of fractured rock. In: Proceedings of the 28th US symposium on rock mechanics, Tucson; 1987. p. 473–80.
[77] Billaux D, Gentier S. Numerical and laboratory studies of flow in a fracture. In: Rock joints: Proceedings of the international symposium on rock joints, Loen, Norway; 1990. p. 369–73.
[78] Makurat A, Barton N, Rad NS, Bandis S. Joint conductivity due to normal and shear deformation. In: Rock joints: Proceedings of the international symposium on rock joints, Loen, Norway; 1990. p. 535–40.
[79] Tsang C-F. Coupled thermo-mechanical hydro-chemical processes in rock fractures. Rev Geophys 1991;29:537–51.
[80] Boulon MJ, Selvadurai APS, Benjelloun H, Feuga B. Influence of rock joint degradation on hydraulic conductivity. Int Rock Mech Min Sci Geomech Abstr 1993;30:1311–7.
[81] Wei L, Hudson JA. A coupled discrete-continuum approach for modelling of water flow in jointed rocks. Geotechnique 1993;43:21–36.
[82] Stephansson O, editor. Proceedings of the international symposium on fundamentals of rock joints, Björkliden, 15–20 September 1985. Lulea (Sweden): Centek; 1985.
[83] Indraratna B, Ranjith PG. Hydromechanical aspects of and unsaturated flow in jointed rock. Leiden: AA Balkema; 2001.
[84] Hopkins DL. The implications of joint deformation in analysing the properties and behaviour of fractured rock masses, underground excavations and faults. Int Rock Mech Min Sci Geomech Abstr 2000;37:175–202.
[85] Selvadurai APS, Voyiadjis GZ, editors. Mechanics of material interfaces. New York: Elsevier; 1986.
[86] Barton N, Stephansson O, editors. Rock joints. Proceedings of the international symposium on rock joints, Loen, Norway; 1990.
[87] Barenblatt GI, Entov VM, Ryzhik VM. Theory of fluid flows through natural rocks. Dordrecht: Kluwer Academic; 1990.
[88] Evans B, Wong T.-f., editors. Fault mechanics and transport properties of rocks. A Festschrift in Honour of W.F. Brace. San Diego: Academic Press; 1992.
[89] Hudson JA, editor. Comprehensive rock engineering, vols. 1–5. New York: Pergamon Press; 1993.
[90] Selvadurai APS, Boulon MJ, editors. Mechanics of geomaterial interfaces. New York: Elsevier; 1995.
[91] Rossmanith H-P, editor. Proceedings of the First International Conference on Damage and Failure of Interfaces, DFI-1, Vienna, Austria, 22–24 September, 1997. Rotterdam (Brookfield, VT, USA): Balkema; 1997.
[92] Bandis SC, Lumsden AC, Barton NR. Fundamentals of rock joint deformation. Int J Rock Mech Min Sci Geomech Abstr 1983;20:249–68.
[93] Drumm E, Fishman K, Zaman M. Modelling of interfaces and joints. In: Modelling in geomechanics. New York: Wiley; 2000. p. 389–426.
[94] Chen W-F. Plasticity in reinforced concrete. New York: McGraw-Hill; 1981.
[95] Chen W-F, Saleeb AF. Constitutive equations for engineering materials, vol. 1. New York: John Wiley; 1982.
[96] Desai CS, Siriwardane HJ. Constitutive laws for engineering materials with emphasis on geologic materials. Englewood Cliffs (NJ): Prentice-Hall; 1984.
[97] Pande GN, Beer G, Williams JR. Numerical methods in rock mechanics. New York: Wiley; 1992.
[98] Darve F, editor. Geomaterials: constitutive equations and modelling. London: Elsevier; 1990.
[99] Pietruszczak S, Pande GN, editors. NUMOG VI, Proceedings of the 7th symposium on numerical models in geomechanics, Montreal; 1997.
[100] Davis RO, Selvadurai APS. Plasticity and geomechanics. Cambridge: Cambridge University Press; 2002.
[101] Davis RO, Selvadurai APS. Elasticity and geomechanics. Cambridge: Cambridge University Press; 1995.
[102] ABAQUS/Standard Version 6.4. ABAQUS Theory Manual. ABAQUS, Inc.; 2004.
[103] Bathe KJ. Finite element procedures. Englewood Cliffs (NJ): Prentice Hall; 1996.
[104] Zienkiewicz OC. The finite element method, 5th ed., vol. 2. Oxford; 2000.
[105] El-Abbasi N, Bathe KJ. Stability and patch test performance of contact discretizations and a new solution algorithm. Comp Struct 2001;79:1473–86.
[106] Wriggers P, Wagner W, editors. Computational mechanics: state of the art. Berlin: Springer-Verlag; 2000.
[107] Willner K. Kontinuums- und kontaktmechanik: Synthetische und analytische darstellung. Berlin: Springer-Verlag; 2003.
[108] Jaeger JC, Cook NGW. Fundamentals of rock mechanics. 2nd ed.. New York: Wiley; 1976.
[109] Selvadurai APS. Partial differential equations in mechanics. The biharmonic equation, Poisson's equation, vol. 2. Berlin: Springer-Verlag; 2000.